Photo-Fenton degradation of malachite green catalyzed by aromatic compounds under visible light irradiation

Feng Chen,[a] Jianjun He,[a] Jincai Zhao*[a] and Jimmy C. Yu[b]

[a] *Laboratory of Photochemistry, Center for Molecular Sciences, Institute of Chemistry, Chinese Academy of Sciences, Beijing 100080, China. E-mail: jczhao@ipc.ac.cn; Fax: +86 10 6487 9375*

[b] *Department of Chemistry, The Chinese University of Hong Kong, Shatin, New Territories, Hong Kong, China*

Received (in Montpellier, France) 13th August 2001, Accepted 14th November 2001
First published as an Advance Article on the web 19th February 2002

The photo-Fenton degradation of malachite green (MG) catalyzed by aromatic derivatives under visible light irradiation was examined. Aromatic derivatives exhibit significant catalytic action in the photo-Fenton reaction. The degradation rates of MG with various kinds of aromatic derivatives obey the following order: hydroquinone > salicylic acid > quinone > carboxylic aromatic derivatives > amido aromatic derivatives. GC-MS detection of the products formed in the MG Fenton degradation in the presence of aromatic derivatives shows that the addition of the latter does not change the MG degradation pathways, although it greatly alters the reaction rate. The MG degradation mainly involves two different pathways: cleavage with a $[MG–OH]^{\bullet}$ transition intermediate and N-demethylation.

The Fenton reaction has been widely studied to treat various kinds of organic pollutants in wastewater[1–4] and was found to effectively degrade almost all kinds of organic compounds through the attack by ${}^{\bullet}OH$ radicals. Recently, the introduction of visible light to dye/Fenton systems has been found to greatly accelerate the Fenton degradation of dye compounds.[5–7] The reaction mechanism of the visible light assisted photo-Fenton process involves the formation of hydroxyl and hydroperoxyl radicals and electron transfer between the excited dyes and the ferric ions:[5–11]

$$Fe^{2+} + H_2O_2 \longrightarrow Fe^{3+} + {}^{\bullet}OH + HO^- \qquad k_1 = 58\ \text{mol}^{-1}\ \text{dm}^3\ \text{s}^{-1} \quad (1)$$

$$Fe^{3+} + H_2O_2 \longrightarrow Fe^{2+} + HO_2^{\bullet} + H^+ \qquad k_2 = 0.02\ \text{mol}^{-1}\ \text{dm}^3\ \text{s}^{-1} \quad (2)$$

$$Fe^{2+} + {}^{\bullet}OH \longrightarrow Fe^{3+} + HO^- \quad (3)$$

$$Fe^{3+} + HO_2^{\bullet} \longrightarrow Fe^{2+} + O_2 + H^+ \quad (4)$$

$${}^{\bullet}OH + H_2O_2 \longrightarrow HO_2^{\bullet} + H_2O \quad (5)$$

$$\text{Dye} \xrightarrow{h\nu} \text{Dye*} \quad (6)$$

$$\text{Dye*} + Fe^{3+} \longrightarrow \text{Dye}^{\bullet+} + Fe^{2+} \quad (7)$$

Cycling of ferrous and ferric ions proceeds through reactions (1) and (2), which continually produce the active radicals (${}^{\bullet}OH$, $HO_2^{\bullet}$). The slow reaction (2) is the rate-determining step of this Fenton process. Any action that promotes the transformation of ferric ions to ferrous ions would help accelerate the Fenton reaction. In the dye/Fenton solution, visible light excites the dye molecules, which then transfer electrons to ferric ions to produce ferrous ions, hence promoting the Fenton reaction.

Addition of other compounds has been found to greatly influence the Fenton degradation of target organic compounds in the dark.[12–15] Aromatic derivatives, such as hydroquinone and hydroquinone-like compounds, were found to have a catalytic action, to greatly promoting the Fenton degradation of organic compounds in the dark.[16–18] Considering that aromatic derivatives are the main pollutants in wastewater and most dye-contaminated wastewaters contain various kinds of aromatic derivatives such as phenol and hydroquinone, a detailed study on their effect on the Fenton and photo-Fenton reactions would be of great importance. However, little work has been done on the behavior of aromatic derivatives in the visible light assisted photo-Fenton degradation of dyes.

This paper shows that aromatic derivatives with different kinds of substituent groups can catalyze the visible light assisted photo-Fenton reaction, and hence promote dye degradation. The effect of the aromatic derivatives depends highly on their different molecular structures. In order to reveal the details of the influence of these aromatic derivatives on the visible light assisted photo-Fenton degradation of dyes, the variations in the concentrations of MG and H_2O_2 in the reaction process were measured and the EPR technique was used to detect the active radicals generated in the reaction solution. To better understand the effect of the aromatic derivatives on the visible light assisted photo-Fenton reaction, addition of inorganic and aliphatic organic compounds was also examined and found to suppress the degradation of MG. The degraded products formed in the visible light assisted photo-Fenton degradation of MG in the presence of quinone were also determined by GC-MS measurements to reveal more details about the mechanism of Fenton degradation of dyes.

DOI: 10.1039/b107404k

Experimental

Materials

Malachite green (MG), salicylic acid, 1,4-hydroquinone, 1,2-hydroquinone, resorcinol, quinone, aniline, *o*-phthalic acid, potassium fluoride, ethylenediaminetetraacetic acid (EDTA), propandioic acid, KH_2PO_4, $Fe(ClO_4)_3 \cdot 9H_2O$ and hydrogen peroxide were of laboratory reagent grade and used without further purification. The spin trap, DMPO, was purchased from Sigma Chemical Co. Deionized and doubly distilled water was used throughout this study.

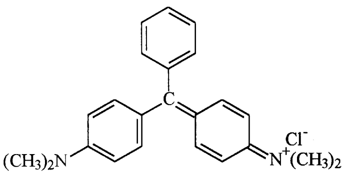

Malachite green (MG)

Photoreactor and light source

A 500 W halogen lamp (Institute of Electric Light Source, Beijing) was positioned inside a cylindrical Pyrex jacket and was cooled by recirculating water. A cutoff filter was placed outside the Pyrex jacket to completely remove wavelengths shorter than 450 nm to ensure that the irradiation only consisted of visible light. The reactor was a cylindrical Pyrex vessel with a volume of 70 ml and was placed at a fixed distance from the light source.

Analytical methods

Reaction solutions were freshly prepared from stock solutions of $Fe(ClO_4)_3$ (5 mmol dm^{-3}) at pH 1.9 and MG (1 mmol dm^{-3}) at pH 4.8 and their pH was adjusted to the desired values with $HClO_4$ and NaOH solutions. Then H_2O_2 was added to the solution to initiate the reaction. At given time intervals, 3.5 ml samples were taken out and their absorbance values at 617 nm (absorption maximum for MG) were recorded with a Lambda Bio20 UV-VIS spectrophotometer (Perkin–Elmer Co.). The GC-MS data were obtained with a Trio-2000 spectrometer, equipped with an SPB5 column, 30 m × 0.32 mm. The sample was prepared as follows: the solvent of the reacted solution was vaporized directly (below 323 K) under reduced pressure. The remaining residue was dissolved in methanol. Changes in the H_2O_2 concentration were determined by a photometric method described in the literature.[19,20] A Brucker Model EPR 300E spectrometer equipped with a Quanta-Ray Nd:YAG laser (355 and 532 nm) was used for measurements of the electron paramagnetic resonance (EPR) signals. The settings were: center field = 3486.7 G, sweep width = 100.0 G, microwave frequency = 9.82 GHz, power = 5.05 mW. To minimize experimental errors, the same quartz capillary tube was used for all EPR measurements.

Results and discussion

Degradation of MG

Fig. 1 displays the degradation of MG (1×10^{-4} mol dm^{-3}) in the presence of the Fe^{3+} (2×10^{-4} mol dm^{-3}) and H_2O_2 (2×10^{-2} mol dm^{-3}) with and without visible light irradiation. Although MG was scarcely decomposed in the Fe^{3+} homogeneous (curve a) and H_2O_2 homogeneous (curve b) solutions, the coexistence of Fe^{3+} and H_2O_2 (Fenton reagent) degraded the MG to some extent (curve c). Both irradiation by visible light and addition of quinone greatly promoted the Fenton degradation of MG (curves d and e), where under both conditions almost all of the MG molecules disappeared in about 80 min. The photo-Fenton degradation of MG under visible light irradiation in the presence of quinone showed a quicker rate, revealing that addition of quinone and visible light irradiation cooperatively promote the Fenton process. Since only MG absorbs the visible light in the solution, the promotion of the visible light assisted photo-Fenton reaction is attributed to an electron transfer between the excited MG and the ferric ions [as shown in eqn. (7)].

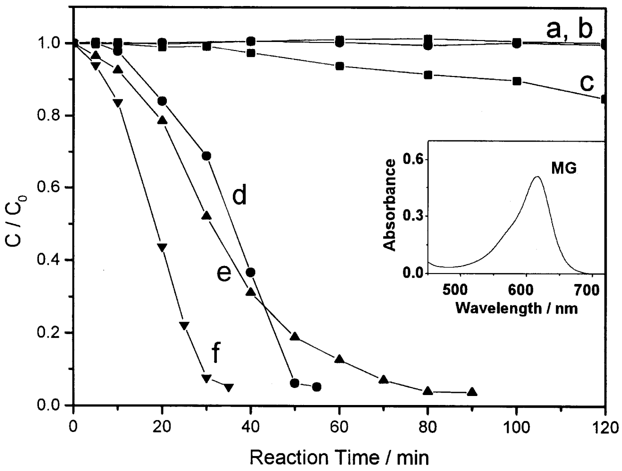

Fig. 1 Degradation of MG under various conditions: (a) in Fe^{3+} solution under visible light irradiation, (b) in H_2O_2 solution under visible light irradiation, (c) in the presence of Fe^{3+} and H_2O_2 in the dark, (d) in the presence of Fe^{3+} and H_2O_2 under visible light irradiation, (e) in the presence of Fe^{3+}, H_2O_2 and quinone in the dark, (f) in the presence of Fe^{3+}, H_2O_2 and quinone under visible light irradiation. MG (1×10^{-4} mol dm^{-3}), H_2O_2 (2×10^{-2} mol dm^{-3}), Fe^{3+} (2×10^{-4} mol dm^{-3}), quinone (5×10^{-5} mol dm^{-3}). The insert shows the UV-vis absorbance spectrum of MG for (f).

The excited MG molecules transfer electrons to the ferric ions to produce ferrous ions, which promote the regeneration of ferrous ions [as does reaction (2)] and accelerates the Fenton reaction. Addition of quinone to the reaction showed similar effects as those observed with visible light irradiation. In a recent study, it was found that addition of aromatic derivatives to the dye/Fenton system enhances the concentration of ferrous ions in the dark.[18] The reaction mechanism of the catalysis of quinone is shown below (the redox potentials of quinone and $HO_2^{\cdot}$(aq) are also indicated to reveal the thermodynamic basis[21,22]):

$$HO_2^{\cdot}(aq) + H^+ + e \rightarrow H_2O_2(aq) \quad 1.44\,V \qquad (8)$$

$$O_2 + H^+ + e \rightarrow HO_2^{\cdot}(aq) \quad -0.046\,V \qquad (9)$$

$$p\text{-quinone} + 2e + 2H^+ \rightarrow p\text{-hydroquinone} \quad 0.6992\,V \qquad (10)$$

$$HO_2^{\cdot} + \text{quinone} \rightarrow \text{semiquinone} + O_2 \qquad k_{11} = 1 \times 10^9\ M^{-1}\,s^{-1} \quad (11)^{22,23}$$

$$HO_2^{\cdot} + \text{semiquinone} \rightarrow \text{hydroquinone} + O_2 \qquad k_{12} = 1 \times 10^9\ M^{-1}\,s^{-1} \quad (12)^{22,23}$$

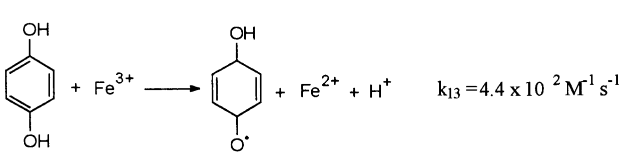

(13)

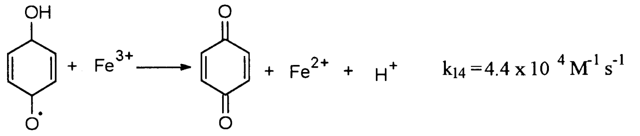

(14)

Although addition of quinone (curve e) promoted the MG degradation more efficiently than visible light irradiation (curve d) in the initial stages of the reaction, its effect abated with continued degradation of MG and was weaker than that of visible light irradiation in the later stages of the MG degradation process. This is due to decomposition of the quinone, lowering its catalytic effect. Accompanying by the decrease in the absorbance of the MG, the maximum of the characteristic absorption peak also moved from 617 nm to 599 nm, which indicates N-demethylation of the MG.

The Fenton degradation of rhodamine 6G was also examined under various conditions. The results were similar to those of MG: the Fenton degradation of rhodamine 6G was accelerated by quinone both in the dark and under visible light irradiation. This indicates that the promotion of the Fenton reaction by quinone is insensitive to the nature of the dye in solution.

MG degradation in the presence of different kinds of compounds

Fig. 2(A) a shows the visible light assisted photo-Fenton degradation of MG (2×10^{-5} mol dm^{-3}) in the presence of different kinds of inorganic compounds. Compared to the control reaction, the degradation rate of MG in the presence of inorganic compounds was slower. This is mainly attributed to complexation of the inorganic compounds with the iron ions, which makes the reaction between iron and H_2O_2 less probable. The photo-Fenton degradation of MG (2×10^{-5} mol dm^{-3}) was also suppressed in the presence of different kinds of aliphatic compounds [as shown in Fig. 2(B)]. Besides forming complexes with iron, these aliphatic compounds may also interact with $^{\cdot}OH$ radicals. The photo-Fenton degradation of MG in the presence of EDTA is an interesting example. Initially, it is very slow due to the strong complexation between iron and EDTA. However, the degradation rate picks up as more free iron ions are released due to the decomposition of EDTA by $^{\cdot}OH$ radicals. The suppression effects of inorganic and aliphatic compounds that we observed are quite similar to those reported for reactions in the dark.[12,18]

Fig. 3 shows the visible light assisted photo-Fenton degradation of MG (2×10^{-5} mol dm^{-3}) in the presence of different kinds of aromatic derivatives. Unlike their inorganic and aliphatic counterparts, these aromatic species generally have a positive influence on the degradation of MG. It has been reported that hydroquinone and related aromatic compounds could catalyze the Fenton degradation of target compounds by directly reducing Fe(III) to Fe(II), while other aromatic derivatives catalyzed the Fenton reaction through the hydroquinone-like degraded products.[14,15,18] Our results show that most aromatic derivatives are also effective catalysts in visible light assisted photo-Fenton reactions. Among the compounds studied, 1,4-hydroquinone and 1,2-hydroquinone are the most effective. Since salicylic acid must be converted to hydroquinone or hydroquinone-like compounds before it catalyzes the photo-Fenton reaction, the catalytic power of salicylic acid is weaker than that of hydroquinone. This was also observed in the presence of resorcinol, which cannot be oxidized directly to quinone because of its structure and hence exhibits a lower catalytic effect than 1,4-hydroquinone and 1,2-hydroquinone. As shown in Fig. 3, the effectiveness of the aromatic derivatives is in the order: hydroquinones > salicylic acid > quinone > resorcinol > carboxylic aromatic derivative > amido aromatic derivative. This series correlates well with the ability to transform to hydroquinone or hydroquinone-like compounds. Since amido aromatic derivatives tend to react with protons to generate ammonium in the acidic solution under the Fenton reaction conditions, they are less likely to undergo electrophilic attack by hydroxyl radicals to transform to

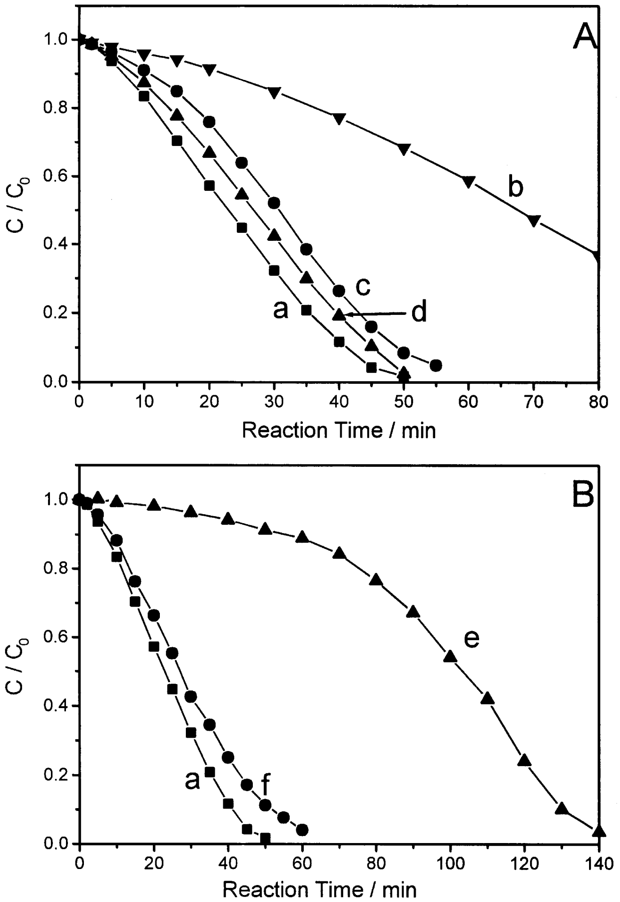

Fig. 2 Fenton degradation of MG: (a) control reaction and in the presence of: (b) $H_2PO_4^-$, (c) F^-, (d) NO_3^-, (e) EDTA, (f) propane diacid. Visible light irradiation, MG (2×10^{-5} mol dm^{-3}), H_2O_2 (2×10^{-3} mol dm^{-3}), Fe^{3+} (2×10^{-4} mol dm^{-3}), other compounds (2×10^{-4} mol dm^{-3}).

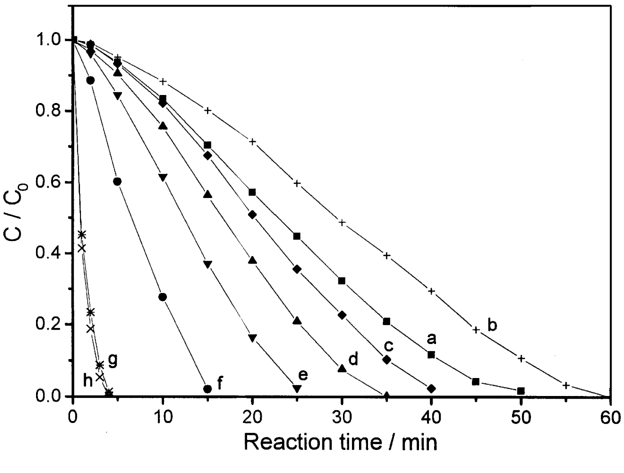

Fig. 3 Fenton degradation of MG: (a) control reaction and in the presence of: (b) aniline, (c) *o*-phthalic acid, (d) resorcinol, (e) quinone, (f) salicylic acid, (g) 1,2-hydroquinone, (h) 1,4-hydroquinone. Visible light irradiation, MG (2×10^{-5} mol dm^{-3}), H_2O_2 (2×10^{-3} mol dm^{-3}), Fe^{3+} (2×10^{-4} mol dm^{-3}), other compounds (2×10^{-5} mol dm^{-3}).

hydroquinone-like compounds. As a result, amido aromatic derivatives do not exhibit catalytic effects in the visible light assisted photo-Fenton reaction. In fact, the MG photodegradation rate in the presence of aniline is even slower than that of the control reaction.

H_2O_2 determination and EPR measurements

The change of H_2O_2 concentration during the Fenton reaction gives some important information about the process. In order to enhance the concentration effects, a relatively low initial H_2O_2 concentration of 4×10^{-4} mol dm^{-3} was used. Fig. 4 shows the H_2O_2 decomposition rate in the presence of EDTA, quinone and salicylic acid. EPR experiments have confirmed that a large amount of hydroxyl radicals are generated in the Fenton reaction.[6,24] Fig. 5 shows the DMPO spin-trapping EPR spectra in the presence of various kinds of compounds. The intensity of the EPR signals correlates well with the Fenton reaction rate. Addition of EDTA, which significantly suppresses the degradation of MG, results in a much weaker EPR intensity of DMPO–$^{\bullet}$OH. On the other hand, the presence of quinone and salicylic acid promotes the generation of $^{\bullet}$OH radicals. The EPR results are also in good agreement with the MG Fenton degradation rates and the extent of H_2O_2 decomposition. Addition of aromatic compounds promotes regeneration of ferrous ions, accelerates the reaction between the iron ions and H_2O_2, and facilitates the generation of $^{\bullet}$OH radicals from decomposition of H_2O_2.

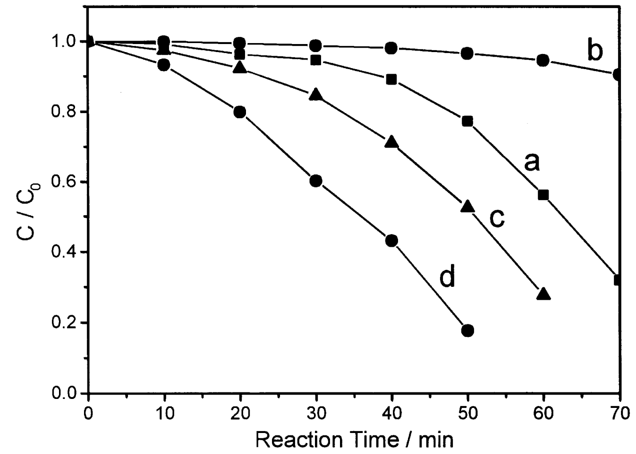

Fig. 4 H_2O_2 concentration variation in (a) the control reaction and in the presence of: (b) EDTA, (c) quinone, (d) salicylic acid. Visible light irradiation, MG (2×10^{-5} mol dm^{-3}), H_2O_2 (4×10^{-4} mol dm^{-3}), Fe^{3+} (2×10^{-4} mol dm^{-3}), other compounds (2×10^{-5} mol dm^{-3}).

GC-MS analysis

Fig. 6 displays the GC-MS chromatograms of the products formed in the Fenton degradation of MG in the presence of quinone under visible light irradiation. The GC peak of MG does not appear since it is too non-volatile for GC separation. Identified degradation products are listed in Table 1 together with their retention times and areas. The most abundant intermediate (peak I, retention time 24.62 min) is 4-dimethylaminobenzophenone, which is generated through the cleavage of the bond between the central carbon atom and the dimethylaminophenyl group. The MS data of 4-dimethylaminobenzophenone are listed in Table 2. Because of the influence of the dimethylamino group, MG tends to fragment at the bond between the central carbon atom and dimethylaminophenyl. Although 4,4′-dimethylaminobenzophenone does not appear in the GC spectra, some analogous degradation products such as 4-dimethylamino-4′-methylaminobenzophenone and 4-dimethylamino-4′-aminobenzophenone are present, indicating that MG also fragments at the bond between the central carbon atom and the phenyl group. Some chlorinated compounds were also detected in the degradation products, suggesting that chlorine radicals are also involved in the degradation of MG. Table 2 lists the MS data of the degradation products.

MG Fenton degradation experiments were also carried out in the presence of quinone but without visible light irradiation. GC-MS measurements show similar degradation products being generated. We believe that the irradiation by visible light does not alter the major MG Fenton degradation pathways. Small amounts of products other than those listed in Table 1 were also detected. They were $HCON(CH_3)_2$, $CH_3OCON(CH_3)_2$, and 4-hydroxylbenzoic acid. We also monitored the change in TOC value during the photo-Fenton degradation of

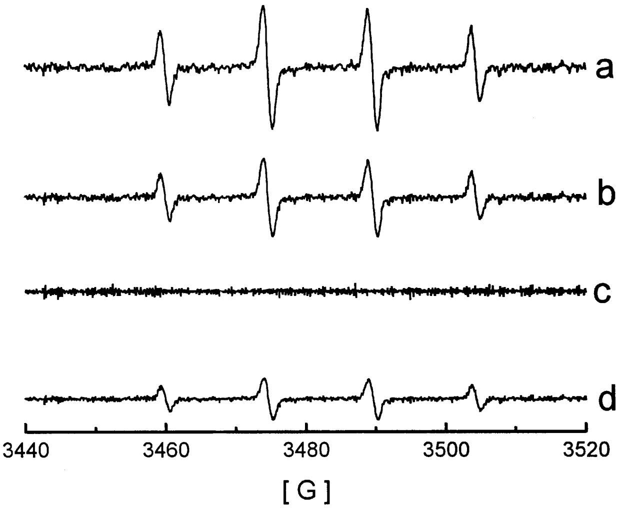

Fig. 5 DMPO spin-trapping EPR spectra of MG/Fenton solution in (a) the control reaction and in the presence of: (b) EDTA, (c) quinone, (d) salicylic acid. Visible light irradiation, MG (1×10^{-4} mol dm^{-3}), H_2O_2 (2×10^{-2} mol dm^{-3}), Fe^{3+} (2×10^{-4} mol dm^{-3}), other compounds (1×10^{-4} mol dm^{-3}).

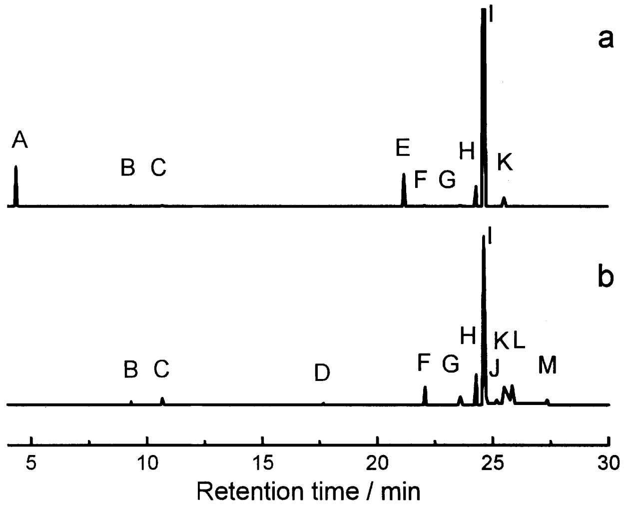

Fig. 6 GC chromatograms of MG Fenton degradation products in the presence of quinone under visible light irradiation: (a) 30% of MG degraded; (b) 90% of MG degraded. The intensity scale in (b) is two times larger than that in (a). Initial concentrations: MG (1×10^{-4} mol dm^{-3}), H_2O_2 (2×10^{-3} mol dm^{-3}), Fe^{3+} (2×10^{-4} mol dm^{-3}), quinone (5×10^{-5} mol dm^{-3}).

Table 1 Retention times and peak areas of the identified degradation products in the visible light assisted photo-Fenton degradation of MG

Peak	Product	Retention time/min	Peak area (%)	
			a	b
A	$HCONHCH_3$	4.37	25.6	0
B	4-Dimethylaminophenol	9.32	0.90	2.50
C	$C_6H_5COONH_4$	10.66	1.25	4.60
D	$(CH_3)_2NC_6H_5COOCH_3$	17.65	0	0.24
E	MW = 211	21.15	22.8	1.33
F	3-Oxo-4-methylimino-1,5-cyclohexadienyl phenone	22.07	1.24	8.98
G	3-Hydroxyl-4-dimethylamino-benzophenone	23.60	5.30	3.11
H	4-Methylaminobenzophenone	24.28	15.2	13.2
I	4-Dimethylaminobenzophenone	24.61	500	100
J	Chloric-4-methylamino-benzophenone	25.16	0	1.85
K	2-Hydroxyl-4-dimethylamino-benzophenone	25.4	10.1	2.23
L	4-Dimethylamino-4′-amino-benzophenone	25.84	0	1.24
M	4-Dimethylamino-4′-methylaminobenzophenone	27.3	0	0.34

Table 2 MS data of the degradation products formed in the visible light assisted photo-Fenton degradation of MG

Peak	m/z (rel. int. of predominant ions in fragmentation pattern, %)
A	59(79); 45(37); 29(80); 15(100)
B	136(5); 105(23); 77(78); 51(100)
C	122(6); 105(15); 77(58); 51(100)
D	179(38); 148(70); 132(22); 118(25); 104(72); 77(75)
E	211(80); 210(765); 194(13);165(79); 152(33); 134(93); 118(57); 91(100)
F	223(8); 146(26); 118(8); 105(43); 90(45); 77(100)
G	241(9); 136(60); 120(5); 105(82); 77(100)
H	211(16); 134(67); 105(21); 91(15); 77(100)
I	225(37); 148(100); 105(32); 91(12); 77(97)
J	247(3); 245(8); 170(8); 168(26); 105(28); 77(100)
K	241(12); 164(14); 121(20); 105(28); 77(100)
L	241(10); 148(11); 121(100); 120(38); 105(14)
M	255(13); 148(16); 134(100); 120(52); 105(17)

MG in the presence of quinone. It changed from 12.38 ppm to 7.58 ppm in 240 min, indicating mineralization of organic compounds.

In a recent study,[25] the degradation products formed in the visible light assisted photo-Fenton degradation of MG without aromatic additives were analyzed by GC-MS. Only five products (*N,N*-dimethylaniline, 4-dimethylaminophenol, 4-methylaminobenzophenone, 4-dimethylaminobenzophenone, 4-hydroxybenzoic acid) were detected. This work identifies many more degradation products and hence more detailed degradation pathways can be postulated. Interestingly, we have found a new pathway in which MG molecules are cleaved at the bond between the central carbon atom and the phenyl group.

Mechanism of the MG degradation

Aromatic derivatives accelerate the photo-Fenton reaction under visible light irradiation but do not alter the degradation pathways for MG degradation. The visible light assisted photo-Fenton degradation of MG in the presence of quinone mainly involves two different pathways as summarized in Scheme 1: cleavage with a $[MG–OH]^•$ transition intermediate and N-demethylation. All of the proposed degradation products have been identified by our GC-MS measurements except those that are highly unstable or too non-volatile for

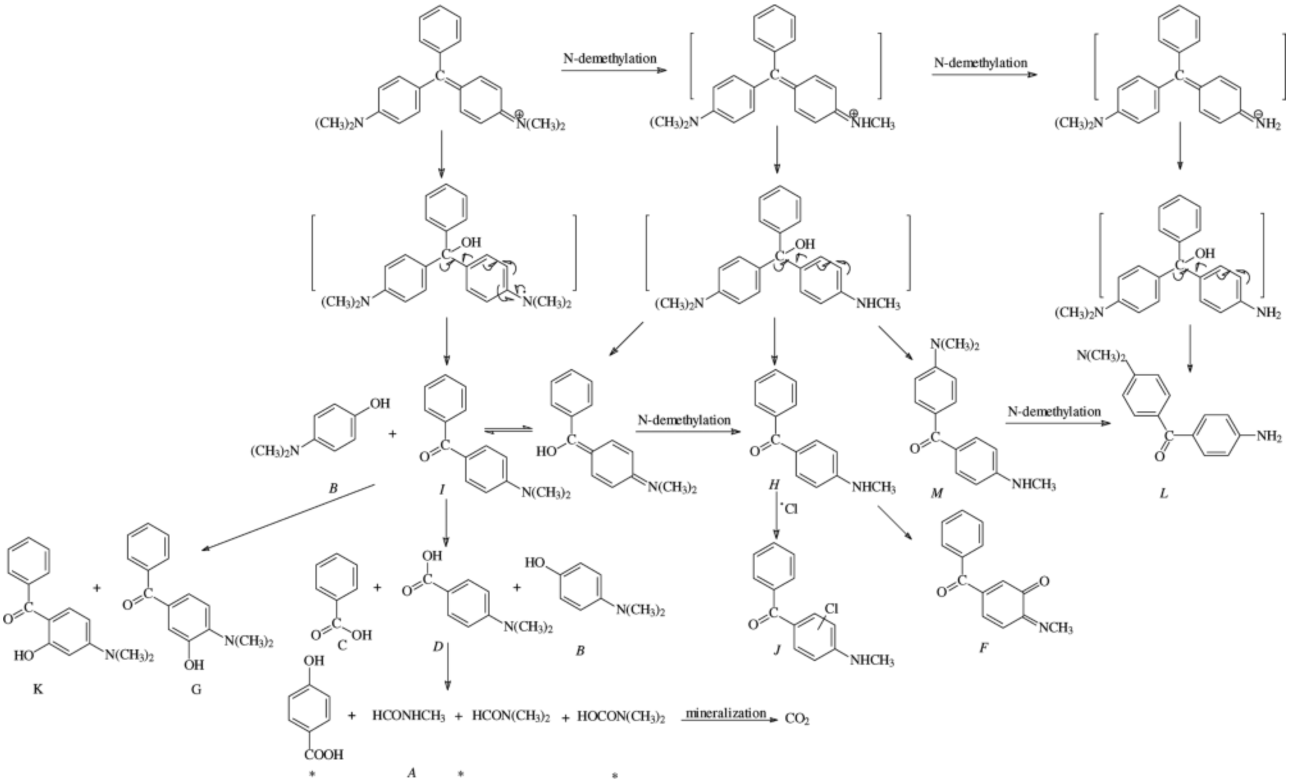

* Identified from the intermediates formed in the Fenton degradation of MG in the presence of quinone in the dark

Scheme 1 MG photo-Fenton degradation pathways in the presence of quinone under visible light irradiation.

GC separation. Because of the influence of the dimethylamino group, the [MG–OH]$^{\bullet}$ transition intermediates are mainly cleaved at the bond between the central carbon atom and dimethylaminophenyl group, and hence 4-dimethylaminobenzophenone is the most abundant intermediate of the MG degradation. The process of N-demethylation is apparent in the UV-Vis spectra of the MG degradation, and is further confirmed by the formation of various N-demethylation degradation products in the GC chromatograms. In either pathway, the breakup of the MG molecule begins with the cleavage of the bonds between the central carbon atom and other groups. This forms numerous products as listed in Table 1. The formation of chlorinated degradation products may be initiated by the reaction between chloride ions and $^{\bullet}$OH. MG molecules were degraded and eventually mineralized in the presence of aromatic additives in the photo-Fenton degradation.

Conclusions

Aromatic derivatives can effectively catalyze the photo-Fenton degradation of MG under visible light irradiation. The catalytic power of aromatic derivatives follows the order: hydroquinones > salicylic acid > quinone > carboxylic aromatic derivative > amido aromatic derivative. The addition of aromatic derivatives does not alter the main MG degradation pathways, which include cleavage with a [MG–OH]$^{\bullet}$ transition intermediate and N-demethylation.

Acknowledgments

This work was supported by the National Natural Science Foundation of China (No. 29877026, No. 20077027, and No. 4001161947), the Foundations of Chinese Academy of Sciences and National Committee of Chinese Science and Technology, and a grant from the NSFC/RGC Joint Research Scheme (N_CUHK433/00).

References

1 W. R. Haeg and C. D. Yao, *Environ. Sci. Technol.*, 1992, **26**, 1005.
2 J. T. Spadaro, L. Zsabelle and V. Renganathan, *Environ. Sci. Technol.*, 1994, **28**, 1389.
3 J. J. Pignatello, *Environ. Sci. Technol.*, 1992, **26**, 944.
4 W. Spacek, R. Bauer and G. Heisler, *Chemosphere*, 1995, **30**, 477.
5 J. Bandeara, C. Marrison, J. Kiwi, C. Plugarin and P. Pevinger, *J. Photochem. Photobiol. A: Chem.*, 1996, **99**, 57.
6 K. Wu, Y. Xie, J. Zhao and H. Hidaka, *J. Mol. Catal.*, 1999, **144**, 77.
7 K. Wu, T. Zhang, J. Zhao and H. Hidaka, *Chem. Lett.*, 1998, **6**, 857.
8 C. Walling and A. Goosen, *J. Am. Chem. Soc.*, 1973, **95**, 2987.
9 W. G. Barb, J. H. Baxendale, P. George and K. R. Hargrave, *Trans. Faraday Soc.*, 1951, **47**, 591.
10 R. G. Zepp, B. C. Faust and J. Hoigne, *Environ. Sci. Technol.*, 1992, **26**, 313.
11 G. Ruppett, R. Bauer and G. Heisier, *J. Photochem. Photobiol. A: Chem.*, 1993, **73**, 75.
12 M. Lu, J. Chen and C. Chang, *Chemosphere*, 1997, **35**, 2285.
13 V. Nadtochenko and J. Kiwi, *Environ. Sci. Technol.*, 1998, **32**, 3282.
14 K. A. Hislop and J. R. Bolton, *Environ. Sci. Technol.*, 1999, **33**, 3119.
15 M. E. Balmer and B. Sulzberger, *Environ. Sci. Technol.*, 1999, **33**, 2418.
16 G. A. Hamilton, J. W. Hanifin and J. P. Friedman, *J. Am. Chem. Soc.*, 1966, **88**, 5269.
17 R. Z. Chen and J. J. Pignatello, *Environ. Sci. Technol.*, 1997, **31**, 2399.
18 F. Chen, W. Ma, J. He and J. Zhao, *Environ. Sci. Technol.*, submitted.
19 Y. Zuo and J. Hoigne, *Science*, 1993, **260**, 71.
20 T. Wu, G. Liu, J. Zhao, H. Hidaka and N. Serpone, *J. Phys. Chem.*, 1999, **103**, 4862.
21 *CRC Handbook of Chemistry & Physics*, ed. R. D. Weast, D. Lide, M. J. Astle and W. H. Beyer, CRC Press, Inc., 70th edn., 1989.
22 *Methods in Enzymology*, ed. L. Packer, Academic Press, Inc., London, vol. 105, 1984.
23 K. B. Patel and R. L. Willson, *J. Chem. Soc., Faraday Trans.*, 1973, **69**, 814.
24 Y. Xie, F. Chen, J. He, J. Zhao and H. Wang, *J. Photochem. Photobiol. A: Chem.*, 2000, **136**, 235.
25 Y. Xie, K. Wu, F. Chen, J. He and J. Zhao, *Res. Chem. Intermed.*, 2001, **27**, 237.